B202

Simulation of Mainshock of 2016 Kumamoto Earthquake Using Dynamic Rupture Modeling

○Jikai SUN, Hiroshi KAWASE, Arben PITARKA, Fumiaki NAGASHIMA

The mainshock of the 2016 Kumamoto earthquake occurred on April 16, 2016 at 01:25 (JST) in the Kyushu Island (Yoshida et al., 2017), on the Futagawa and Hinagu fault system. The Mw magnitude of the earthquake was 7.0. The kinematic rupture modeling of the Kumamoto earthquake was applied in several studies (e.g., Yoshida et al., 2017; Asano and Iwata, 2021) to investigate the rupture process and simulate the strong ground motion for the mainshock. Near-fault ground motions generated by the earthquake were recorded with high accuracy by the NIED strong-motion network (K-NET and Kik-net), the Japan Meteorological Agency (JMA), and the local-government seismic-intensity network (Irikura et al., 2020).

In this study, we used dynamic rupture modeling (Pitarka et al., 2021) to investigate the earthquake rupture and simulate the recorded near fault ground motions. The dynamic rupture is modeled using the split-node method of Dalguer and Day (2007), implemented in the 3D staggered-grid finite-difference method of Pitarka (1999) and a linear slip-weaking friction law (e.g., Andrews, 1976). Following the slip models of Yoshida et al. (2017) and Asano and Iwata (2021) we generated 500 and 858 stress drop rupture models with three strong motion generation areas (SMGAs) with elevated stress drop, located on the Futagawa and Hinagu fault zones. The location of the SMGAs were randomly generated in the large slip distribution areas (Figs. 1 and 2). The 3D Japan integrated velocity structure model (JIVSM) (Koketsu et al., 2008, 2012) was used in modeling the elastic wave propagation. Then, a linear regression method was applied to the eight end points of four fault segments, to define the location of 45 km long rupture plane (Fig. 3). The top-left and bottom-right boundaries were determined by 13 km offset from the rupture plane (the blue line), the bottom-left and top-right boundaries were offset 10 and 5 km from the outmost-edge foot points on the linear regression line. We simulated the ground motion at 26 strong-motion stations belonging to the JMA and K-NET/KiK-net networks. We used the misfit of PGV and cross-correlation coefficient (CCC) between the recorded and synthetic strong-ground motions at each site among 1358 scenarios, to isolate the rupture model that best fit the waveforms at 26 sites. The synthetic waveforms compare very well with the recorded ones at 16 of 26 sites. Moreover, a series of combination parameters consisted of PGV misfit and CCC with different weighting factors were tested to find the best-fit scenario. Figure 4 shows the rupture scenario No. 0174 that best fit the recorded data at most of the sites. We performed additional simulations focused on testing the effect of the rake angle on the quality of synthetic ground motion. Rupture scenarios with rake angles between 20 and 30 degree performed relatively better. Thus, we concluded that the rake angle of the mainshock was in this range, which means that the northwest plate sink 20 degree towards the northeast direction. This is consisted with the previous research results (e.g., Yoshida et al, 2017; Asano and Iwata, 2021).

Reference

Andrews, D. J., 1976, JGR, 81, 5679–5687.

Asano, K., and T. Iwata, 2021, BSSA, doi: 10.1785/0120210047.

Dalguer, L. A., and S. M. Day, 2007, JGR: Solid Earth, 112, no. B2, doi: 10.1029/2006JB004467.

Irikura, K., S. Kurahashi, and Y. Matsumoto, 2020, PAG, 177, no. 5, 2021–2047, doi: 10.1007/s00024-019-02283-4.

Koketsu, K., H. Miyake, H. Fujiwara, and T. Hashimoto, 2008, in 14WCEE Beijing.

Koketsu, K., H. Miyake, and H. Suzuki, 2012, in 15WCEE Lisboa.

Pitarka, A., 1999, BSSA, 89, no. 1, 54–68.

Pitarka, A. et al., 2021, BSSA, doi: 10.1785/0120210138.

Yoshida, K. et al, 2017 EPS, 69, no. 1, doi: 10.1186/s40623-017-0649-8.

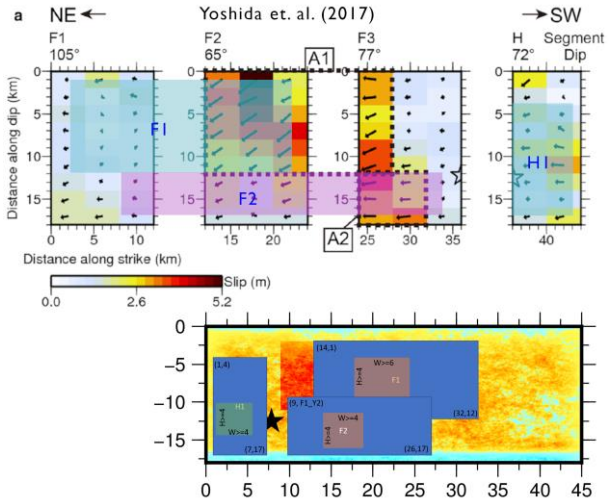

Fig.1 Randomly generate locations of SMGA based on results of Yoshida et al. (2017)

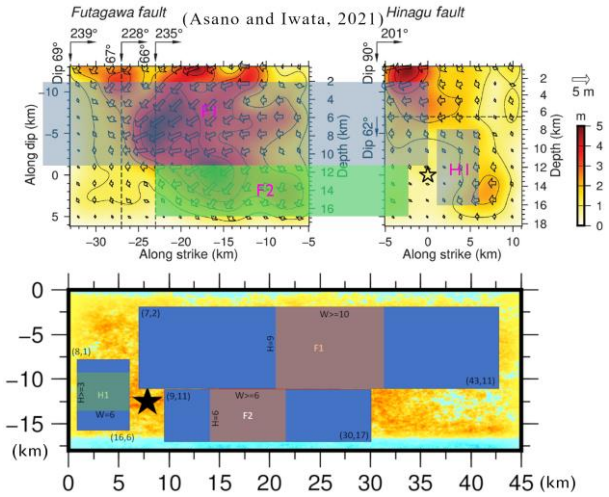

Fig. 2 Randomly generate locations of SMGA based on results of Asano and Iwata (2021)

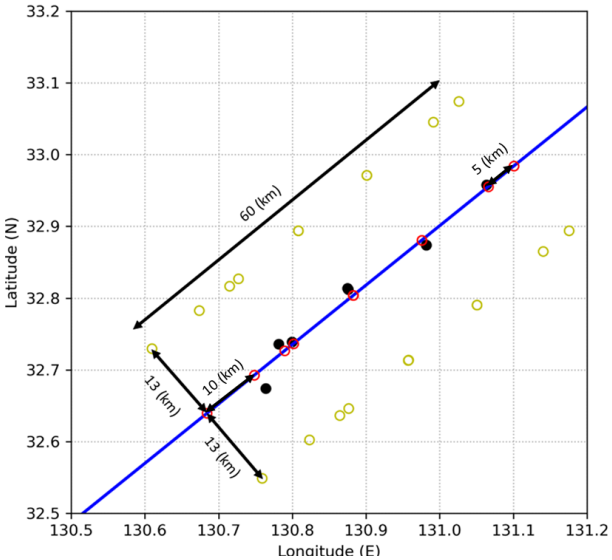

Fig. 3 Location of fault plane in rupture dynamic modeling. Black, red, and yellow circles denote the end points of fault segments, foot positions, and boundary points, respectively

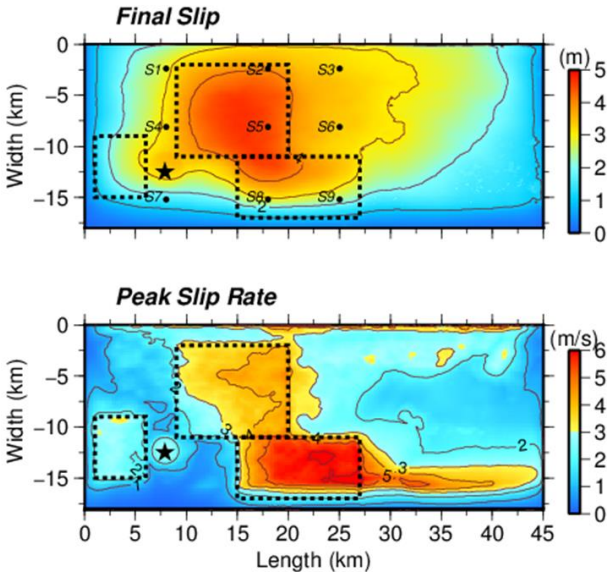

Fig. 4 Rupture dynamic results of No. 0174. Top and bottom panels display the distributions of final slip and peak slip rate during the mainshock